AGU PUBLICATIONS

Geophysical Research Letters

RESEARCH LETTER

10.1002/2017GL073869

Key Points:
- Meridional OLR gradient over Africa is a skillful predictor of seasonal Atlantic hurricane activity
- The African OLR gradient has been strengthening (weakening) since (prior to) ~1980s, due to anthropogenic greenhouse gases (aerosols)
- The African OLR gradient is projected to continue increasing in the future, suggesting more frequent Atlantic hurricanes

Supporting Information:
- Supporting Information S1

Correspondence to:
L. Zhang,
lezh8230@colorado.edu

Citation:
Zhang, L., T. Rechtman, K. B. Karnauskas, L. Li, J. P. Donnelly, and J. P. Kossin (2017), Longwave emission trends over Africa and implications for Atlantic hurricanes, *Geophys. Res. Lett., 44*, 9075–9083, doi:10.1002/2017GL073869.

Received 18 APR 2017
Accepted 17 AUG 2017
Accepted article online 22 AUG 2017
Published online 9 SEP 2017

Longwave emission trends over Africa and implications for Atlantic hurricanes

Lei Zhang[1], Thomas Rechtman[2,3], Kristopher B. Karnauskas[1,4], Laifang Li[5], Jeffrey P. Donnelly[6], and James P. Kossin[7]

[1]Cooperative Institute for Research in Environmental Sciences, University of Colorado Boulder, Boulder, Colorado, USA, [2]University of Central Florida, Orlando, Florida, USA, [3]SMART Program, University of Colorado Boulder, Boulder, Colorado, USA, [4]Department of Atmospheric and Oceanic Sciences, University of Colorado Boulder, Boulder, Colorado, USA, [5]Earth and Ocean Sciences, Nicholas School of the Environment, Duke University, Durham, North Carolina, USA, [6]Department of Geology and Geophysics, Woods Hole Oceanographic Institution, Woods Hole, Massachusetts, USA, [7]Center for Weather and Climate, NOAA National Centers for Environmental Information, Madison, Wisconsin, USA

Abstract The latitudinal gradient of outgoing longwave radiation (OLR) over Africa is a skillful and physically based predictor of seasonal Atlantic hurricane activity. The African OLR gradient is observed to have strengthened during the satellite era, as predicted by state-of-the-art global climate models (GCMs) in response to greenhouse gas forcing. Prior to the satellite era and the U.S. and European clean air acts, the African OLR gradient weakened due to aerosol forcing of the opposite sign. GCMs predict a continuation of the increasing OLR gradient in response to greenhouse gas forcing. Assuming a steady linear relationship between African easterly waves and tropical cyclogenesis, this result suggests a future increase in Atlantic tropical cyclone frequency by 10% (20%) at the end of the 21st century under the RCP 4.5 (8.5) forcing scenario.

1. Introduction

There is an average of about 12 named tropical storms per year over the Atlantic Ocean [*Karnauskas and Li*, 2016 (KL16)], all of which have the potential to significantly impact property and population in the region. Atlantic seasonal hurricane activity prediction is thus of great societal interest. The genesis and maximum potential intensity of tropical cyclones (TCs) is controlled by several factors including local sea surface temperature (SST), large-scale low-level vorticity, midlevel humidity, upper tropospheric (outflow) temperature, and the magnitude of vertical wind shear [*Gray*, 1979; *Emanuel*, 2010]. Remote forcing, such as the El Niño–Southern Oscillation (ENSO), influences climate conditions over the Atlantic and therefore also plays an important role in driving change in Atlantic hurricane activity [*Bell and Chelliah*, 2006].

Karnauskas [2006] and KL16 found that the Atlantic seasonal hurricane activity is closely associated with the meridional gradient of outgoing longwave radiation (OLR) over Africa. The physical connection between the OLR gradient and tropical storms is as follows: (a) the meridional OLR gradient reflects the temperature gradient between Sahara Desert and central Africa, which is the main driver of the African easterly jet [*Hsieh and Cook*, 2008]; (b) the OLR difference between central and northern/southern Africa is closely connected with the strength of the intertropical convergence zone (ITCZ), which is further related to the local Hadley circulation [*Zhang and Wang*, 2013]. Hence, a stronger meridional OLR gradient over Africa indicates stronger instabilities associated with the easterly wave production, which may serve as seeds for Atlantic TCs [*Thorncroft and Hodges*, 2001; *Hopsch et al.*, 2010], although the linear relationship between African easterly waves (AEWs) and Atlantic TCs also depends on large-scale conditions and is thus not always steady [e.g., *Ross et al.*, 2012]. The African hydroclimate has been singled out as an important driver of Atlantic hurricane activity in the past [*Gray*, 1990; *Donnelly and Woodruff*, 2007]. However, it has also been noted in previous studies that the relationship between Sahel rainfall and Atlantic TC activity may have changed, yielding to the failure of the African rainfall predictor for Atlantic TCs [*Klotzbach*, 2007; *Fink et al.*, 2010; *Caron et al.*, 2012; *Klotzbach et al.*, 2015; *Boudreault et al.*, 2017]. Nevertheless, using an OLR index in July as the only predictor, which is the OLR averaged over northern and southern Africa minus that over central Africa, KL16 showed that the prediction of named Atlantic storms yields a success rate of 87% during 2001–2015, compared to 53% success rate of prediction from the U.S. National Oceanic and Atmospheric Administration (NOAA) over the same period.

KL16 noted that the July African OLR trend observed by satellite projects strongly onto the OLR anomaly pattern associated with named Atlantic storms. Given the close association between the African meridional OLR gradient and Atlantic hurricane activity, natural questions are (a) how significant is the observed trend in African OLR during the satellite era, (b) what are physical causes of the OLR trends, and (c) how will the meridional OLR gradient evolve in the future? In this study, we address these three questions, which are important for understanding future changes in Atlantic storms and especially their potential impacts on coastal landforms, ecosystems, societies, and economies.

2. Observational Data and Climate Models

We employ satellite observations of OLR from NOAA over the period 1979–2015 [*Liebmann and Smith*, 1996]. OLR from the National Centers for Environmental Prediction Reanalysis 2 (NCEP2) data set over the same period was also analyzed [*Kanamitsu et al*., 2002]. Because of the limited period of the satellite observations, OLR during 1900–2014 from the twentieth century reanalysis data version 2c (20CRv2c) was used [*Compo et al*., 2011]. The HURricane DATa second generation data set from NOAA was also employed [*Landsea and Franklin*, 2013].

To determine the cause of the recent observed OLR trend, historical simulations for the period 1900–2005 from 30 global climate models from the Coupled Model Intercomparison Project Phase 5 (CMIP5) were analyzed (Table S1in the supporting information). We also examine future projections for the period 2006–2100 under Representative Concentration Pathway (RCP) 4.5 and 8.5 scenarios to explore future African OLR trends. In addition, single forcing experiments for the period 1900–2005, i.e., experiments with anthropogenic aerosol (AA) forcing or greenhouse gas (GHG) forcing only, provided by 11 CMIP5 models were analyzed to examine relative roles of the two primary anthropogenic forcings in the African OLR trend (Table S1). In the following section, we will present and analyze the ensemble mean of CMIP5 models. Interested readers may refer to Table S1 and Figures S1–S4 for CMIP5 details.

3. Results

As previously shown by *Karnauskas* [2006] and KL16, the seasonal number of named Atlantic storms is tightly linked with the meridional structure of African OLR (Figure 1a), with more storms being associated with positive OLR anomalies over northern and southern Africa and a negative OLR anomaly over central Africa. The strengthened meridional OLR gradient indicates a stronger temperature gradient between northern and central Africa and an enhanced ITCZ/regional Hadley circulation, both of which can contribute to jet instabilities and easterly wave production. Following KL16, we focus on the OLR trend in July, given that July is the complete month after which Atlantic seasonal hurricane predictions (June–November) are issued by NOAA annually. Results of the trend pattern, attribution and future projection of African OLR for the entire hurricane season are similar (not shown).

The African OLR trend pattern observed by satellite (1979–2015) projects strongly onto that of the OLR anomaly pattern regressed onto named Atlantic hurricanes (Figure 1b), with a strengthening meridional OLR gradient in recent decades. OLR trends from 20CRv2c also exhibit an enhanced meridional gradient (Figure 1d). It has been proposed that such an observed OLR trend pattern may contribute to observed trends in Atlantic storms [KL16]. Interestingly, a very similar OLR trend pattern to satellite observations is captured by the CMIP5 historical ensemble over the same period (Figure 1c), despite a much smaller magnitude. Because the ensemble-mean approach may effectively filter out the randomly distributed internal climate variabilities across different models, this result implies that the recent strengthening African meridional OLR gradient may be attributable to external forcing.

To explore the time evolution of the African meridional OLR gradient, we define an OLR index, which is the average of domain-mean OLR over northern and southern Africa minus that over the central Africa (boxes marked in Figure 1). Regions chosen to calculate OLR indices in this study are slightly modified compared to the ones used in KL16 to focus on diagnosing the OLR trend pattern from CMIP5 future projections rather than simply the covariability with named storms, but OLR anomalies in these modified boxes are still closely aligned with the OLR anomaly pattern associated with Atlantic hurricanes. In this study, we refer to the meridional OLR gradient as the magnitude of OLR gradient between north (Sahara) and central Africa (ITCZ) as well as that between central and South Africa, and the OLR index represents the peakedness in the African

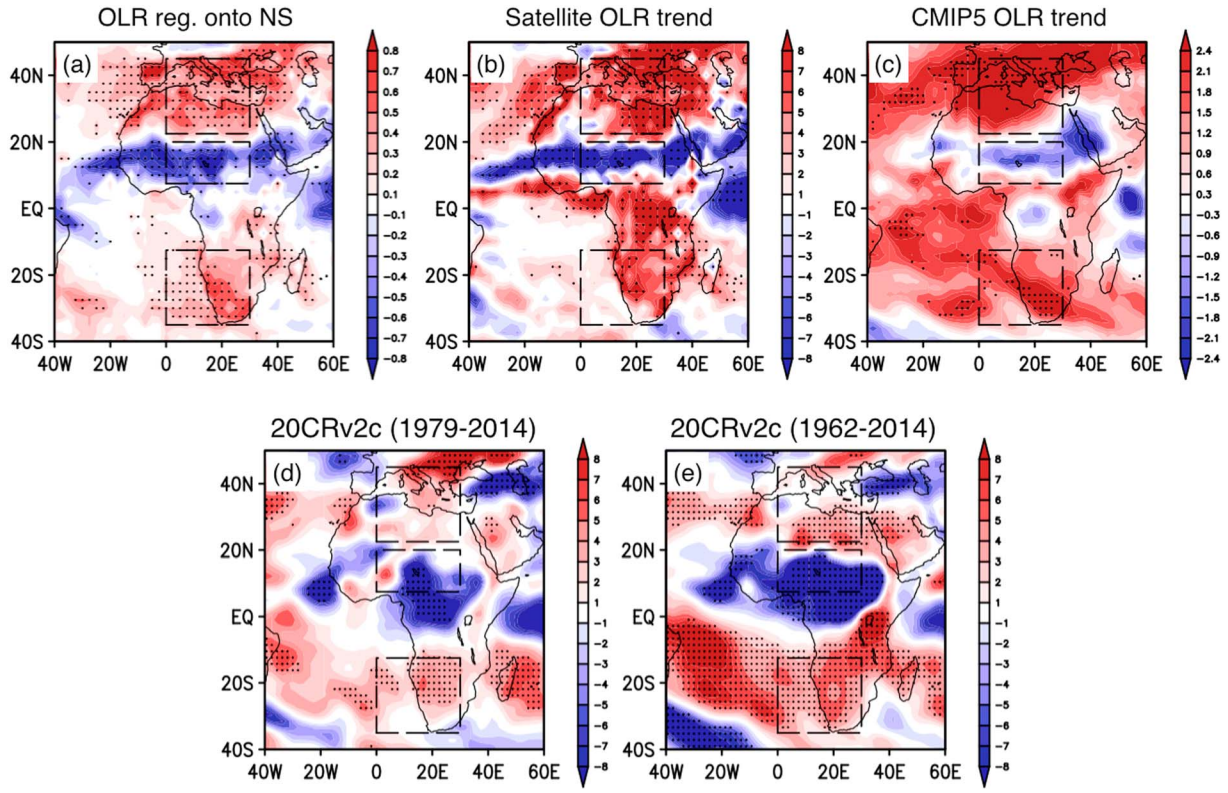

Figure 1. (a) Regression of July OLR onto number of named storms (June–November) during 1979–2015 (W m^{-2} per number of named storms). (b) Observed July OLR trend by satellite during 1979–2015 (W m^{-2} 37 yr^{-1}). (c) As in Figure 1b but for multimodel mean OLR trend during 1979–2015 from 30 CMIP5 models (W m^{-2} 37 yr^{-1}). (d and e) As in Figure 1b but for OLR trend in 20CRv2c during 1979–2014 and 1962–2014, respectively. Units are W m^{-2} 36 yr^{-1} in Figure 1d and W m^{-2} 53 yr^{-1} in Figure 1e. The year 1962 is when the 20CRv2c OLR index reaches minimum (Figure 2a). Note that scales of color bars in Figures 1b and 1c are different. Stippling denotes the region that is 90% statistically significant in Figures 1a, 1b, 1d, and 1e and 24/30 model agreement in Figure 1c. Boxes denote regions for defining the OLR index, which are 22.5°N–45°N, 0–30°E; 7.5°N–20°N, 0–30°E; 35°S–12.5°S, 0–30°E.

OLR. Consistent with the strengthening meridional OLR gradient observed by satellites, the OLR index calculated using the satellite data set exhibits a significant increasing trend during 1979–2015 (0.23 W m^{-2} yr^{-1}, 95% statistically significant) (Figures 2a and S1). The OLR index from the NCEP2 reanalysis exhibits a slightly greater increasing trend compared to satellite observations, while the OLR index trend is smaller in 20CRv2c than that observed by satellite. The CMIP5 multimodel mean result also shows a small but positive trend in the OLR index during the satellite era, with a relatively large intermodel spread. The 40-member ensemble of fully coupled Community Earth System Model (CESM) simulations exhibit very similar results to CMIP5 models (Figure S1). The spread of the projected change in the OLR index may be associated with different phases of internal variabilities across different models/ensemble members. It is also interesting that the OLR index trend in satellite observations is very close to the high end of the projected OLR index trend in climate models (Figure S1). These results suggest that the magnitude mismatches between satellite observations and CMIP5 models may relate to decadal variabilities being filtered out in the CMIP5 multimodel mean result. Roles of internal and external forced variabilities in Atlantic TC decadal variabilities have indeed been noted in previous studies [*Camargo et al.*, 2013; *Ting et al.*, 2015].

To extend the OLR index beyond the satellite era, we use the 20CRv2c data set, and we applied a 72 year low-pass filter (twice the length of the satellite era) to remove the influence of interannual and decadal variabilities. The stronger trend of the African meridional OLR gradient observed by satellites than that in the 20CRv2c appears to be due to a stronger positive OLR trend over northern Africa/southern Europe in the satellite data compared to the 20CRv2c (Figures 1 and 2b). Also interesting is that the strengthened OLR index in the NCEP2 is primarily due to a decrease in OLR over the ITCZ, which is different from satellite observations (not shown). Furthermore, the 20CRv2c OLR index suggests that the recent strengthening OLR gradient trend over Africa began ~17 years prior to the satellite era, prior to which there was an overall negative

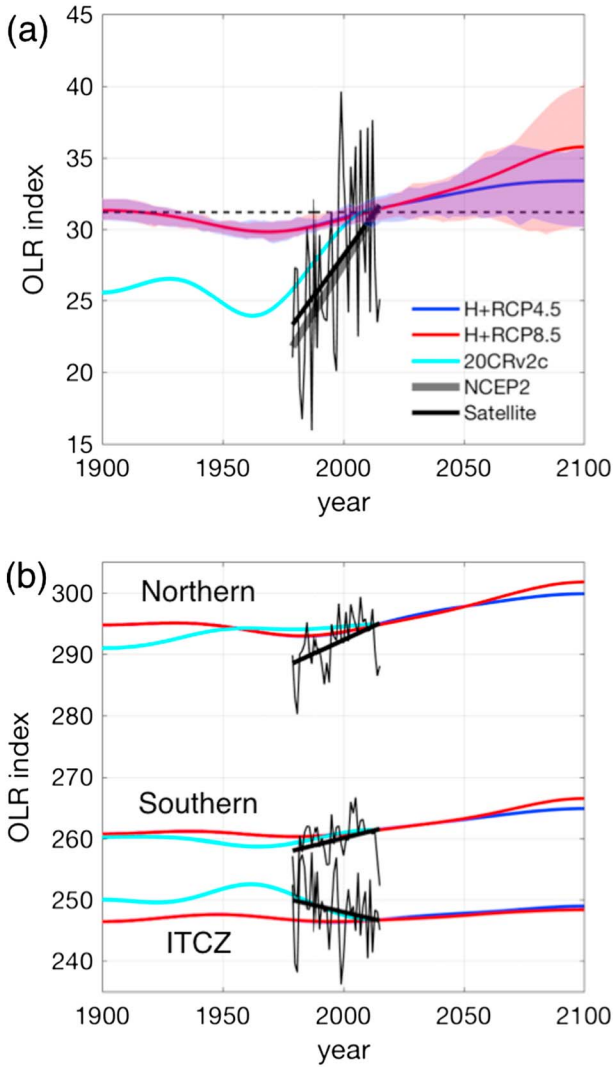

Figure 2. (a) Time evolution of the OLR index from satellite observation (black), 20CRv2c (cyan), NCEP2 (linear trend, gray), and CMIP5 models. Red (blue) for historical simulation during 1900–2005 and RCP8.5 (RCP4.5) experiments for the period 2006–2100. Shading represents uncertainty across different CMIP5 models, which is defined as the 25th (lower boundary) and 75th percentile (upper boundary) (blue for RCP4.5, red for RCP8.5). (b) As in Figure 2a but for the OLR averaged over northern, central, and southern Africa. OLR indices in 20CRv2c and CMIP5 models are 72 year low-pass filtered, and the linear trend of OLR index in satellite observation is shown. The indices are centralized toward the trend line value in the year 2014 in satellite observations.

trend in the OLR index with noticeable decadal variabilities (Figures 1 and 2a). This is consistent with previous studies that found a drying (wetting) trend over Sahel before (after) the 1980s [*Held et al.*, 2005; *Fontaine et al.*, 2011; *Dong and Sutton*, 2015]. The decreasing meridional OLR gradient during early twentieth century suggested by the 20CRv2c and the increasing trend observed by satellite in recent decades are both predicted by CMIP5 historical simulations (Figure 2a). This result suggests that the centennial scale trend of the African meridional OLR gradient is primarily attributable to the external forcing. However, similar to the satellite era, trends since 1900 are also stronger in the 20CRv2c than in the CMIP5 multimodel mean result.

To explore roles of the external forcing in the African OLR trend during the two intervals, we analyzed CMIP5 single forcing experiments for the two primary anthropogenic forcings, i.e., AAs and GHGs. Consistent with the OLR index evolution, OLR trend patterns from CMIP5 historical runs prior to and after 1979 are indeed opposite (Figures 3a and 3b), featuring weakening and strengthening of the meridional OLR gradient, respectively. Single-forcing experiments suggest that increasing AA (GHG) concentration tend to induce weakening (strengthening) of the meridional OLR gradient (Figures 3d and 3f), which is consistent with findings in previous studies [*Douville et al.*, 2002; *Biasutti and Giannini*, 2006; *Paeth and Feichter*, 2006]. Previous studies also found that AAs (GHGs) contribute to decreasing (increasing) Atlantic TCs [*Ting et al.*, 2015; *Sobel et al.*, 2016]. The decreasing trend of the Africa OLR gradient over the period 1900–1978 is primarily due to the AA forcing dominating the GHG forcing. Note that the AA effect during 1979–2005 is opposite to what it was prior to 1979, which is associated with decreasing AAs over Africa after the 1980s [*Takemura*, 2012; *Dunstone et al.*, 2013; *Dong and Sutton*, 2015]. Consequently, the strengthening OLR gradient during 1979–2005 is due to a combination of changes in both the AA forcing and the GHG forcing (Figures 3c and 3e). Also, note that the OLR trend due to the GHG effect is much smaller during 1900–1978 compared to recent decades (Figures 3e and 3f), which is associated with smaller GHG forcing during the early period. We also note that the summation of the OLR trends induced by AAs and GHGs is greater than that in historical

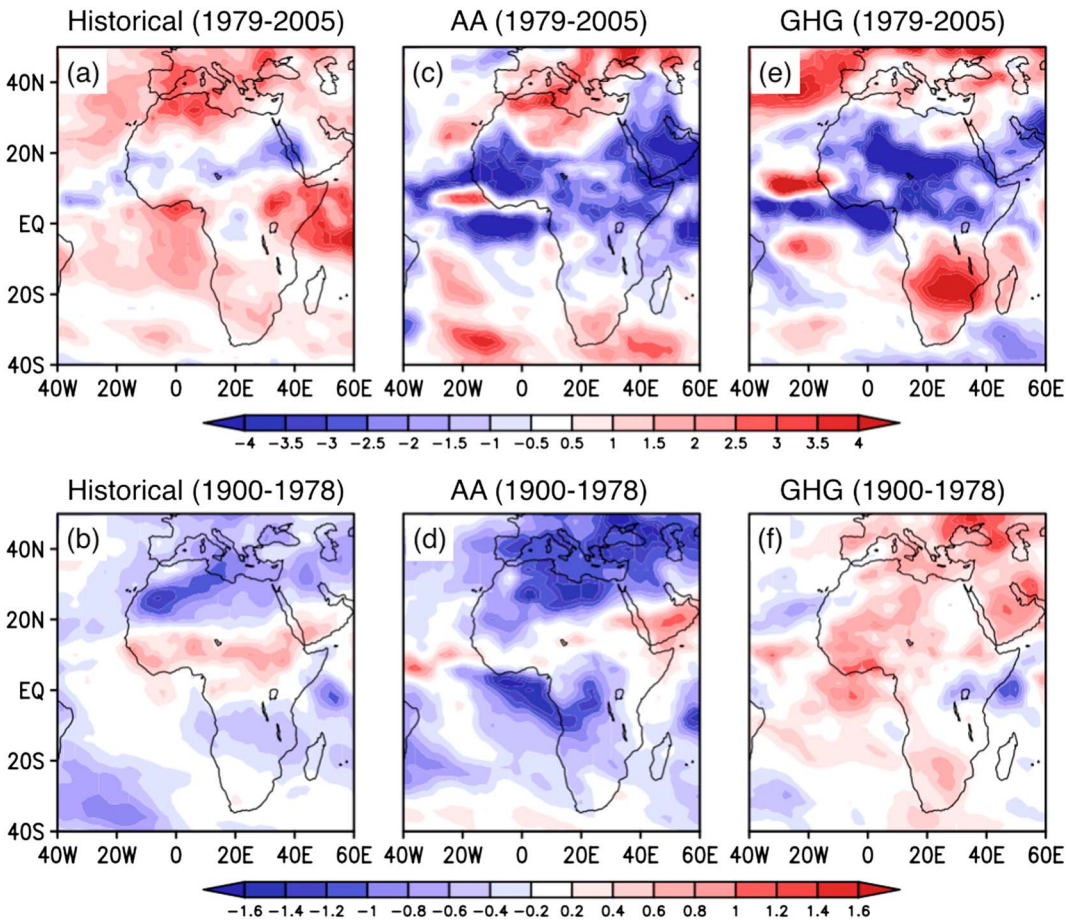

Figure 3. (a) Multimodel mean OLR trend from CMIP5 historical simulations during 1979–2005. (b) As in Figure 3a but for 1900–1978. (c and d) For AA forcing-only experiments, and (e and f) for GHG forcing-only experiments. Units are W m^{-2} 30 yr^{-1}.

simulations, in which both effects are included simultaneously. This discrepancy may be associated with the two anthropogenic forcings acting nonlinearly [*Ming and Ramaswamy*, 2009].

We further analyzed CMIP5 future projections to explore the response of the African OLR gradient to the anthropogenic GHG forcing in the future. RCP8.5 projections predict a continuation of the increasing OLR gradient in CMIP5 historical simulations, including the magnitude of the increasing trend out to 2100 (Figures 2a and 4a). Similar for RCP4.5 simulations except for a smaller magnitude and a leveling-off of the increasing trend by midcentury because of the slowdown of the increasing radiative forcing (Figures 2a and S2a). The largest regional contributions to the future strengthening OLR index are from Northern Africa/Southern Europe and southern Africa (Figures 2b, 4a, and S2a), which differ from satellite observations (during the satellite era, the decrease in ITCZ was about the same as the increase in Sahara, which is due to an expansion of the dry zone and the narrowing of the ITCZ region [*Lau and Kim*, 2015; *Zhang and Li*, 2016]).

Diagnostics of future OLR increases over northern and southern Africa in RCP8.5 experiments suggest that increasing surface temperature plays a leading role (Figure 4c), which induces an enhanced meridional temperature gradient between northern/southern and central Africa. Future OLR also decreases slightly over the ITCZ, which is due to a strengthening and poleward shift of the ITCZ associated with a shift and expansion of the Hadley circulation (Figures 4b, 4d, and S3). The precipitation increases over the ITCZ region despite the local descending motion anomaly, which may be related to the greater moisture availability in a warmer climate (Figures 4b and 4d). Surface temperature beneath the ITCZ increases a small amount, but the increased precipitation dominates the OLR response.

The meridional OLR gradient over Africa and the genesis of tropical waves (i.e., seeds for Atlantic TC genesis) are mechanistically connected. Indeed, the July OLR index and named Atlantic storms (June to November)

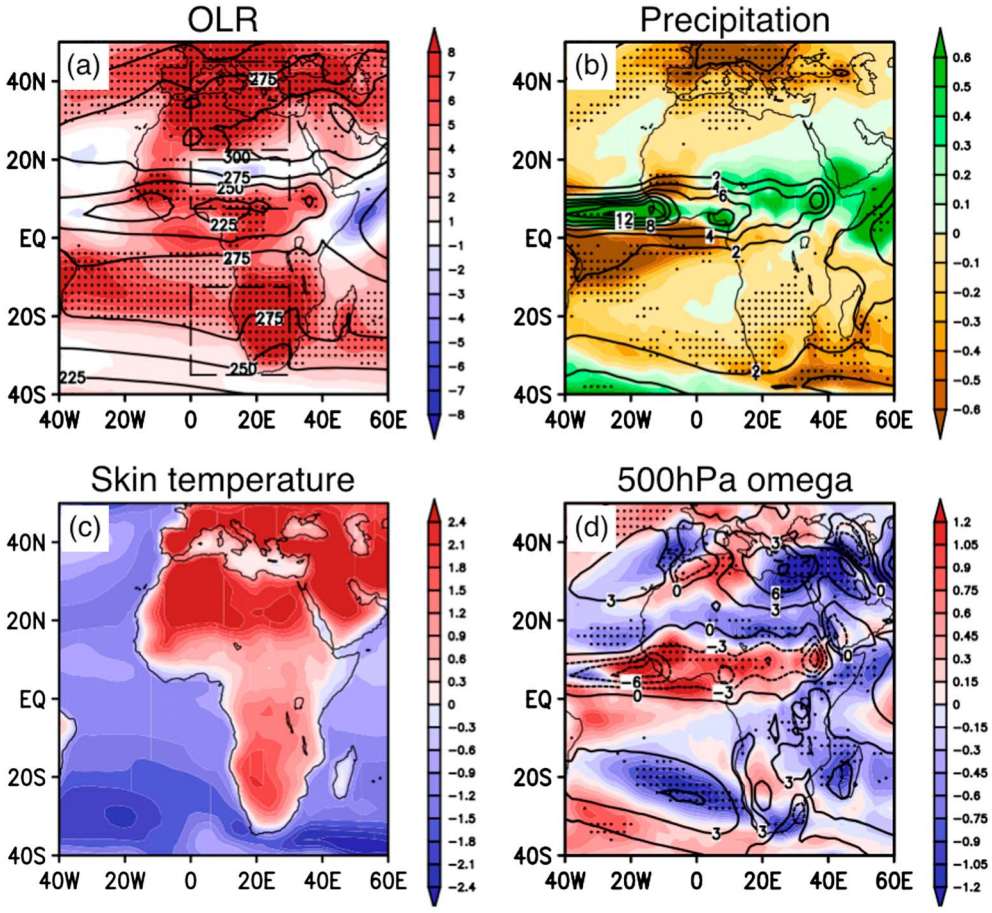

Figure 4. (a) Multimodel mean OLR trend from RCP8.5 experiments (shading, W m^{-2} $century^{-1}$) and OLR climatology (contour, W m^{-2}). (b) As in Figure 4a but for precipitation (units are mm d^{-1} $century^{-1}$ for the trend and mm d^{-1} for climatology). (c) For skin temperature (K $century^{-1}$, domain mean warming removed) and (d) for 500 hPa omega (units are 0.01 Pa s^{-1} $century^{-1}$ for the trend and 0.01 Pa s^{-1} for climatology). Stippling denotes 24/30 model agreement.

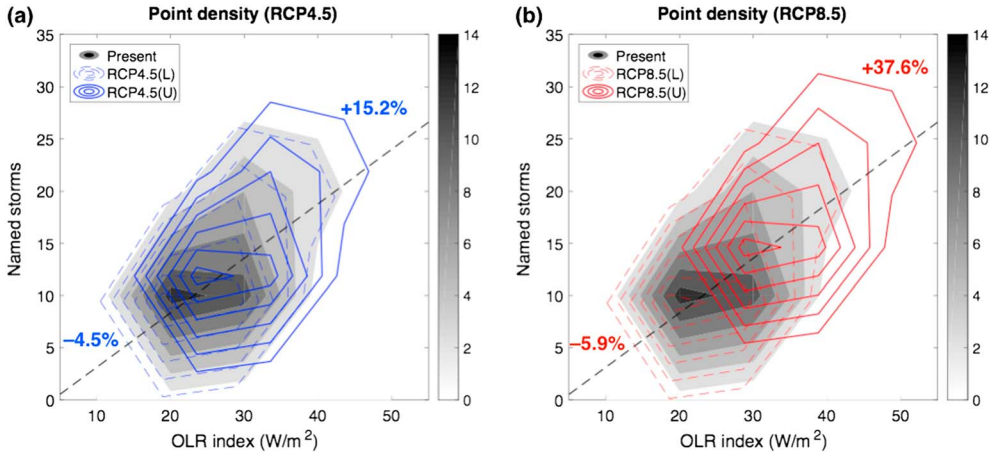

Figure 5. Point density distribution of satellite observed OLR index against number of named Atlantic storms (June–November) during 1979–2015 (shading). Contours denote the point density distribution associated with OLR index change predicted by CMIP5 future projections ((a) for RCP4.5 and (b) for RCP8.5). Dashed (solid) contours are associated with the 25th (75th) percentile of the projected OLR index change.

are highly correlated during the satellite era (correlation coefficient ~0.66, 99% statistically significant). The linear relationship between two variables is determined empirically based on observational data sets during 1979–2015 (slope ~0.52 TCs per W m^{-2}) (Figure 5). Given that physics for the jet instability should not be strongly climate dependent and that TC genesis requires an ambient disturbance [*Gray*, 1979] (although some studies suggest that genesis might also occur spontaneously [*Nolan*, 2007]), it is plausible that the relationship between the strength of the African meridional OLR gradient and the number of named Atlantic storms is stationary and thus can be applied to the future climate. One can then infer that the number of named Atlantic storms would shift toward higher values based on the projected increase in the OLR index. However, several previous studies have suggested a decrease in TC frequency in the future due to changes in large-scale environmental parameters in the main development region (MDR) [*Knutson et al*., 2010]. Our results are largely independent of those parameters and suggest that an increase in seeds for Atlantic TCs may partially compensate for such a decrease due to large-scale conditions over the tropical Atlantic. Under the RCP8.5 forcing scenario, the ensemble-mean OLR index is projected to increase by around 4.7 W m^{-2} by the end of the century, which would imply that the number of named Atlantic storms per year will increase by ~2.4 named storms (or +20%). The ensemble-mean change in the RCP4.5 is about half the magnitude (Figure 2). Although approximately two thirds of CMIP5 models project increases in the African OLR gradient, the uncertainty is relatively large (Figures 5 and S4), which leads to similarly large uncertainty in implied changes in TCs based on OLR changes alone.

4. Conclusion and Discussion

We found a significant strengthening of the African meridional OLR gradient in satellite and reanalysis during 1979–2015. The African OLR trend observed by satellites is predicted as a response to anthropogenic forcing by CMIP5 models, although satellite trends in OLR are ~5 times of those predicted by the CMIP5 multimodel mean, which may be because of natural variabilities being filtered out by the ensemble mean approach.

The 20CRv2c reanalysis suggests that the recent strengthening of the African meridional OLR gradient began in the 1960s, prior to which there was an opposite trend. Multimodel mean results from CMIP5 historical simulations capture a similar evolution of the OLR gradient, despite a smaller magnitude. Analysis of CMIP5 single-forcing experiments reveals that the increasing trend of the OLR index during the satellite era is due to a combination of the GHG forcing and the AA forcing, whereas the decreasing trend of the OLR gradient over 1900–1978 is due to the AA forcing being opposite to what it was since 1979 and stronger in magnitude than the GHG forcing [*Sobel et al*., 2016]. It is worth noting that land use change may also contribute to the observed OLR trends during the satellite era, the role of which cannot be distinguished in the present modeling framework but deserves further attention in the future.

CMIP5 projections predict a continuation of the strengthening OLR gradient in response to future GHG forcing. Diagnostic analysis reveals that the future African OLR trend is due to increasing skin temperature and poleward shifting precipitation over the ITCZ. Under RCP8.5 (4.5), the projected future OLR change would suggest that the number of seeds for Atlantic TC genesis per year will increase by 20% (10%) by the end of the century, assuming that the relationship between the OLR gradient and the number of "seeds" is stationary (physics of jet instability is not climate dependent). If one considers constraints on the total seasonal hurricane activity to be proportional to the number of seeds, modulated by environmental parameters related to their growth into full TCs, our results are addressing the former constraint. Thus, our results are synergistic—not in contrast to—previous studies that explore the latter constraints on TC genesis, which have been shown to be climate dependent (e.g., nonstationarity of the SST threshold for genesis) [*Vecchi and Soden*, 2007]. However, many previous studies [e.g., *Ross et al*., 2012] have found that the linear relationship between AEWs and Atlantic TCs do not always hold, and whether AEWs will develop into TCs or not depend on many other conditions such as their characteristics [*Agudelo et al*., 2011] and/or large-scale environment conditions [*Peng et al*., 2012; *Daloz et al*., 2012; *Satoh et al*., 2013; *Leppert et al*., 2013; *Brammer and Thorncroft*, 2015; *Asaadi et al*., 2016], and how they interact with other waves [*Ventrice et al*., 2011]. This is a caveat that one needs to bear in mind when interpreting our results. Previous work has shown that storms that form from easterly waves are more likely to intensify to major hurricanes and are more likely to threaten multiple coastal regions along their tracks [*Kossin et al*., 2010]. Hence, results shown here underscore the profound societal implications of climate change and concomitant changes in TCs.

Acknowledgments
The 20CRv2c data are provided by the NOAA/OAR/ESRL PSD from their website at http://www.esrl.noaa.gov/psd/. Support for the 20CRv2c data set is provided by the U.S. Department of Energy, Office of Science Biological and Environmental Research, and by the NOAA Climate Program Office. J.P.D., K.B.K., and L.Z. Acknowledge support from the Strategic Environmental Research and Development Program (SERDP) (RC-2336). SERDP is the environmental science and technology program of the U.S. Department of Defense (DoD) in partnership with the U.S. Department of Energy (DOE) and the U.S. Environmental Protection Agency (EPA).

References

Agudelo, P. A., C. D. Hoyos, J. A. Curry, and P. J. Webster (2011), Probabilistic discrimination between large-scale environments of intensifying and decaying African easterly waves, *Clim. Dyn.*, *36*, 1379–1401, doi:10.1007/s00382-010-0851-x.

Asaadi, A., G. Brunet, and M. K. Yau (2016), On the dynamics of the formation of the Kelvin Cat's-Eye in tropical cyclogenesis. Part I: Climatological investigation, *J. Atmos. Sci.*, *73*, 2317–2338, doi:10.1175/JAS-D-15-0156.1.

Bell, G. D., and M. Chelliah (2006), Leading tropical modes associated with interannual and multidecadal fluctuations in North Atlantic hurricane activity, *J. Clim.*, *19*(4), 590–612, doi:10.1175/JCLI3659.1.

Biasutti, M., and A. Giannini (2006), Robust Sahel drying in response to late 20th century forcings, *Geophys. Res. Lett.*, *33*, L11706, doi:10.1029/2006GL026067.

Boudreault, M., L.-P. Caron, and S. J. Camargo (2017), Reanalysis of climate influences on Atlantic tropical cyclone activity using cluster analysis, *J. Geophys. Res. Atmos.*, *122*, 4258–4280, doi:10.1002/2016JD026103.

Brammer, A., and C. D. Thorncroft (2015), Variability and evolution of African easterly wave structures and their relationship with tropical cyclogenesis over the eastern Atlantic, *Mon. Weather Rev.*, *143*, 4975–4995, doi:10.1175/MWR-D-15-0106.1.

Camargo, S. J., M. Ting, and Y. Kushnir (2013), Influence of local and remote SST on North Atlantic tropical cyclone potential intensity, *Clim. Dyn.*, *40*(5–6), 1515–1529, doi:10.1007/s00382-012-1536-4.

Caron, L.-P., C. G. Jones, P. A. Vaillancourt, and K. Winger (2012), On the relationship between cloud–radiation interaction, atmospheric stability and Atlantic tropical cyclones in a variable-resolution climate model, *Clim. Dyn.*, *40*(5–6), 1257–1269, doi:10.1007/s00382-012-1311-6.

Compo, G. P., et al. (2011), The twentieth century reanalysis project, *Q. J. R. Meteorol. Soc.*, *137*(654), 1–28, doi:10.1002/qj.776.

Daloz, A. S., F. Chauvin, K. Walsh, S. Lavender, D. Abbs, and F. Roux (2012), The ability of general circulation models to simulate tropical cyclones and their precursors over the North Atlantic main development region, *Clim. Dyn.*, *39*, 1559–1576, doi:10.1007/s00382-012-1290-7.

Dong, B., and R. Sutton (2015), Dominant role of greenhouse-gas forcing in the recovery of Sahel rainfall, *Nat. Clim. Change*, *5*(8), 757–760, doi:10.1038/nclimate2664.

Donnelly, J. P., and J. D. Woodruff (2007), Intense hurricane activity over the past 5,000 years controlled by El Niño and the West African monsoon, *Nature*, *447*(7143), 465–468.

Douville, H., F. Chauvin, S. Planton, J. F. Royer, D. Salas-Mélia, and S. Tyteca (2002), Sensitivity of the hydrological cycle to increasing amounts of greenhouse gases and aerosols, *Clim. Dyn.*, *20*(1), 45–68, doi:10.1007/s00382-002-0259-3.

Dunstone, N. J., D. M. Smith, B. B. B. Booth, L. Hermanson, and R. Eade (2013), Anthropogenic aerosol forcing of Atlantic tropical storms, *Nat. Geosci.*, *6*(7), 534–539, doi:10.1038/ngeo1854.

Emanuel, K. (2010), Tropical cyclone activity downscaled from NOAA-CIRES reanalysis, 1908–1958, *J. Adv. Model. Earth Syst.*, *2*, 1–12, doi:10.3894/JAMES.2010.2.1.

Fink, A. H., J. M. Schrage, and S. Kotthaus (2010), On the potential causes of the nonstationary correlations between west African precipitation and Atlantic hurricane activity, *J. Clim.*, *23*(20), 5437–5456, doi:10.1175/2010JCLI3356.1.

Fontaine, B., P. Roucou, M. Gaetani, and R. Marteau (2011), Recent changes in precipitation, ITCZ convection and northern tropical circulation over North Africa (1979–2007), *Int. J. Climatol.*, *31*, 633–648.

Gray, W. M. (1990), Strong association between West African rainfall and US landfall of intense hurricanes, *Science*, *249*(4974), 1251–1256.

Gray, W. M. (1979), Hurricanes: Their formation, structure and likely role in the tropical circulation, in *Meteorology Over the Tropical Oceans*, edited by D. B. Shaw, pp. 155–218, R. Meteorol. Soc., Bracknell, U. K.

Held, I. M., T. L. Delworth, J. Lu, K. U. Findell, and T. R. Knutson (2005), Simulation of Sahel drought in the 20th and 21st centuries, *Proc. Natl. Acad. Sci. U.S.A.*, *102*, 17,891–17,896.

Hopsch, S. B., C. D. Thorncroft, and K. R. Tyle (2010), Analysis of African easterly wave structures and their role in influencing tropical cyclogenesis, *Mon. Weather Rev.*, *138*(4), 1399–1419, doi:10.1175/2009MWR2760.1.

Hsieh, J.-S., and K. H. Cook (2008), On the instability of the African easterly jet and the generation of African waves: Reversals of the potential vorticity gradient, *J. Atmos. Sci.*, *65*(7), 2130–2151, doi:10.1175/2007JAS2552.1.

Kanamitsu, M., W. Ebisuzaki, J. Woollen, S. K. Yang, J. J. Hnilo, M. Fiorino, and G. L. Potter (2002), NCEP-DOE AMIP-II Reanalysis (R-2), *Bull. Am. Meteorol. Soc*, *83*, 1631–1643.

Karnauskas, K. B. (2006), The African meridional OLR contrast as a diagnostic for Atlantic tropical cyclone activity and implications for predictability, *Geophys. Res. Lett.*, *33*, L06809, doi:10.1029/2005GL024865.

Karnauskas, K. B., and L. Li (2016), Predicting Atlantic seasonal hurricane activity using outgoing longwave radiation over Africa, *Geophys. Res. Lett.*, *43*, 7152–7159, doi:10.1002/2016GL069792.

Klotzbach, P. J. (2007), Revised prediction of seasonal Atlantic Basin tropical cyclone activity from 1 August, *Weather Forecast.*, *22*(5), 937–949, doi:10.1175/WAF1045.1.

Klotzbach, P., W. Gray, and C. Fogarty (2015), Active Atlantic hurricane era at its end?, *Nat. Geosci.*, *8*(10), 737–738, doi:10.1038/ngeo2529.

Knutson, T. R., J. L. McBride, J. Chan, K. Emanuel, G. Holland, C. Landsea, I. Held, J. P. Kossin, A. K. Srivastava, and M. Sugi (2010), Tropical cyclones and climate change, *Nat. Geosci.*, *3*(3), 157–163, doi:10.1038/ngeo779.

Kossin, J. P., S. J. Camargo, and M. Sitkowski (2010), Climate modulation of North Atlantic hurricane tracks, *J. Clim.*, *23*(11), 3057–3076, doi:10.1175/2010JCLI3497.1.

Landsea, C. W., and J. L. Franklin (2013), Atlantic hurricane database uncertainty and presentation of a new database format, *Mon. Weather Rev.*, *141*(10), 3576–3592, doi:10.1175/MWR-D-12-00254.1.

Lau, W. K. M., and K.-M. Kim (2015), Robust Hadley circulation changes and increasing global dryness due to CO_2 warming from CMIP5 model projections, *Proc. Natl. Acad. Sci. U.S.A.*, *112*(12), 3630–3635, doi:10.1073/pnas.1418682112.

Leppert, K. D., D. J. Cecil, and W. A. Petersen (2013), Relation between tropical easterly waves, convection, and tropical cyclogenesis: A Lagrangian perspective, *Mon. Weather Rev.*, *141*, 2649–2668, doi:10.1175/MWR-D-12-00217.1.

Liebmann, B., and C. A. Smith (1996), Description of a complete (interpolated) outgoing longwave radiation dataset, *Bull. Am. Meteorol. Soc.*, *77*, 1275–1277.

Ming, Y., and V. Ramaswamy (2009), Nonlinear climate and hydrological responses to aerosol effects, *J. Clim.*, *22*(6), 1329–1339, doi:10.1175/2008JCLI2362.1.

Nolan, D. S. (2007), What is the trigger for tropical cyclogenesis?, *Aust. Meteorol. Mag.*, *56*(4), 241–266.

Paeth, H., and J. Feichter (2006), Greenhouse-gas versus aerosol forcing and African climate response, *Clim. Dyn.*, *26*(1), 35–54, doi:10.1007/s00382-005-0070-z.

Peng, M. S., B. Fu, T. Li, and D. E. Stevens (2012), Developing versus nondeveloping disturbances for tropical cyclone formation. Part I: North Atlantic, *Mon. Weather Rev.*, *140*, 1047–1066, doi:10.1175/2011MWR3617.1.

Ross, R. S., T. N. Krishnamurti, and S. Pattnaik (2012), Interactions of diabatic heating in convective superbursts with energy conversion processes in the genesis of Cape Verde hurricanes from African easterly waves, *Mon. Weather Rev.*, *140*(3), 748–773, doi:10.1175/2011MWR3621.1.

Satoh, M., R. Nihonmatsu, and H. Kubokawa (2013), Environmental conditions for tropical cyclogenesis associated with African easterly waves, *SOLA*, *9*, 120–124, doi:10.2151/sola.2013-027.

Sobel, A. H., S. J. Camargo, T. M. Hall, C.-Y. Lee, M. K. Tippett, and A. A. Wing (2016), Human influence on tropical cyclone intensity, *Science*, *353*(6296), 242–246, doi:10.1126/science.aaf6574.

Takemura, T. (2012), Distributions and climate effects of atmospheric aerosols from the preindustrial era to 2100 along representative concentration pathways (RCPs) simulated using the global aerosol model SPRINTARS, *Atmos. Chem. Phys.*, *12*(23), 11,555–11,572, doi:10.5194/acp-12-11555-2012.

Thorncroft, C., and K. Hodges (2001), African easterly wave variability and its relationship to Atlantic tropical cyclone activity, *J. Clim.*, *14*(6), 1166–1179, doi:10.1175/1520-0442(2001)014<1166:AEWVAI>2.0.CO;2.

Ting, M., S. J. Camargo, C. Li, and Y. Kushnir (2015), Natural and forced North Atlantic hurricane potential intensity change in CMIP5 models*, *J. Clim.*, *28*(10), 3926–3942, doi:10.1175/JCLI-D-14-00520.1.

Vecchi, G. A., and B. J. Soden (2007), Effect of remote sea surface temperature change on tropical cyclone potential intensity, *Nature*, *450*(7172), 1066–1070, doi:10.1038/nature06423.

Ventrice, M. J., C. D. Thorncroft, and P. E. Roundy (2011), The madden-Julian Oscillation's influence on African easterly waves and downstream tropical cyclogenesis, *Mon. Weather Rev.*, *139*, 2704–2722, doi:10.1175/MWR-D-10-05028.1.

Zhang, L., and T. Li (2016), Relative roles of anthropogenic aerosols and greenhouse gases in land and oceanic monsoon changes during past 156 years in CMIP5 models, *Geophys. Res. Lett.*, *43*, 5295–5301, doi:10.1002/2016GL069282.

Zhang, G., and Z. Wang (2013), Interannual variability of the Atlantic Hadley circulation in boreal summer and its impacts on tropical cyclone activity, *J. Clim.*, *26*(21), 8529–8544, doi:10.1175/JCLI-D-12-00802.1.